Catálisis, cinética y reactores

Revista Mexicana de Ingeniería Química
Vol. 14, No. 3 (2015) 691-701

SnO_2:Agn THIN FILMS PREPARED BY SOL-GEL APPLIED AS PROPANE GAS SENSORS

PELÍCULAS DELGADAS SnO_2:Agn PREPARADAS POR SOL-GEL APLICADAS COMO SENSORES DE GAS PROPANO

S. Tirado Guerra*

Escuela Superior de Física y Matemáticas, Instituto Politécnico Nacional, U.P. "A.L.M.", San Pedro Zacatenco, C.P. 07738, México, D. F., México

Received April 8, 2015; Accepted July 14, 2015

Abstract

SnO_2 thin films were fabricated by the sol-gel process and repeated immersion technique and deposited on soda-lime substrates. Tin chloride was used as precursor of tin, a 0.2 M solution in 2-methoxyethanol as a solvent and the monoethanolamine as a stabilizer was prepared. From silver nitrate a solution in ethanol was prepared and superficially incorporated onto SnO_2 films, thus obtaining SnO_2:Agn, where n = 0, 1, 3, 5 and 10 times impregnated with silver solution. A series of samples of approximately 150 nm thickness were prepared and were studied. Several layers of Ag were applied superficially on SnO_2 films. The thin films thus obtained are characterized by their structure, XRD, morphology by SEM and chemical composition by EDS, grain shape and size, porosity and surface roughness by AFM, and their electrical and optical (UV-Vis). Properties of SnO_2:Agn samples to propane gas detection in the range of 0-500 ppm gas concentration were tested operating at temperatures of 23, 100, 200 and 300 °C. The results of a selection of these sensors are presented in this paper.

Keywords: thin films, tin dioxide, sol-gel, gas sensors, propane.

Resumen

Películas delgadas de SnO_2 fueron crecidas sobre sustratos de vidrio sodo-cálcico empleando la técnica de sol-gel y el procedimiento de inmersión repetida. De cloruro de estaño se preparó una solución a 0.2 M en 2-metoxietanol y la monoetanolamina como estabilizador. La serie de películas preparadas SnO_2 resultaron de un espesor de 150 nm aproximadamente. Una vez preparadas dichas películas se modificaron superficialmente depositando nanopartículas de plata, a partir de una solución a baja concentración de nitrato de plata en etanol, empleando la técnica de depósito mencionada anteriormente, obteniendo así la serie SnO_2:Agn, con n = 0, 1, 3, 5 y 10, que indica el número de veces que fueron impregnadas con la solución de plata. Ambas series de películas se caracterizaron en su estructura por DRX, morfología por MEB y composición química por EDS, la forma y el tamaño de grano, así como la porosidad y rugosidad por MFA, sus propiedades eléctricas por cuatro y dos puntas, y las ópticas por UV-Vis. Para la serie de películas SnO_2:Agn se determinaron sus propiedades como sensores del gas propano en el rango de concentración de 0-500 ppm y operando a temperaturas de 23, 100, 200 y 300 ºC. Los resultados de una selección de sensores se presentan en este trabajo.

Palabras clave: películas delgadas, dióxido de estaño, sol-gel, sensores de gases, propano.

1 Introduction

Among the metal oxides with different types of applications are the SnO_2 and ZnO, mainly because of its low cost, they are not toxic, stability and especially the natural abundance (Jie, *et al*., 2006; Shinde, *et al*., 2007), both semiconductors, are wide and direct band with values 3.6 and 3.3 eV, respectively (Suchea, *et al*., 2006; Suleimanpour, *et al*., 2011; Schmid, *et al*., 2004; Schmid, *et al*., 2003; Kappler, *et al*., 2001) and exhibit n-type conduction.

Several types of alcohols, gases such as CO, NO_x, H_2, CH_4, C_3H_8, both reducing and oxidizing, some of them are poisonous while other explosives, are

* *Corresponding author. E-mail*: tirado@esfm.ipn.mx
Tel.: +55 57296000 Ext.: 55424 Fax.: +55 57296000 Ext.: 55015

found in environments like the home, in industry and in the automotive environment and can be detected by using the oxides as SnO_2 and ZnO (Jie, *et al*., 2006; Shinde, *et al*., 2007; Suchea, *et al*., 2006), instead of oxides such as TiO_2, MoO_3 (Carriazo *et al*., 2014; Álvarez-Amparán *et al*., 2014), which are used too as catalysts in photo-degradation. Films of ZnO and SnO_2 pure, as well as those modified with noble metals like, Pd, Pt, Ag, Cu, are used as catalysts or as gas sensors (Padilla, *et al*., 2013; Colin-Luna *et al*., 2013; Jie, *et al*., 2006; Shinde, *et al*., 2007; Suchea, *et al*., 2006; Safanova, *et al*., 2001; Li, *et al*., 1999; Matshushima, *et al*., 2003; Shewale, *et al*., 2013; Haridas, *et al*., 2008; Maldonado, *et al*., 2010; Yang, *et al*., 2014; Chizhov, *et al*., 2014). The doped or modified sensors are most commonly used (Schmid, *et al*., 2004; Schmid, *et al*., 2003; Kappler, *et al*., 2001; Fort, *et al*., 2007). The sputtering is a physical method of manufacturing thin films, that it is expensive (Suchea, *et al*., 2006; Sahner, *et al*., 2008; Jianping, *et al*., 2000) and on the other hand are the chemical techniques as spray pyrolysis (Shewale, *et al*., 2013; Maldonado, *et al*., 2010), electrospray (Matshushima, *et al*., 2003), sol-gel (Jie, *et al*., 2006), which are used in the manufacture of thin film sensors, the latter techniques are more accessible, easy, economic and non-toxic. Propane gas sensors based on the films ZnO:Cr prepared by spray pyrolysis (Maldonado, *et al*., 2009) has been reported previously. In this work, SnO_2 thin films were prepared and also those films with surface modified with Ag layers by the sol-gel process and the dip-coating technique (Ilican, *et al*., 2008; Thongsuriwong, *et al*., 2013), in an equipment homemade and where process is controlled by a PC. So, pure SnO_2 films and those with surface modified, SnO_2:Agn, with n = 0, 1, 3, 5 and 10 layers of Ag as catalyst, were characterized and also tested as sensors of propane gas (C_3H_8). The concentrations of the gas used were 0, 1, 5, 50, 100, 200, 300, 400 and 500 ppm. The sensors were tested at operating temperatures of 23, 100, 200 and 300 °C. The matrixes $S(C)_T$ and $S(T)_C$ of sensitivity for a selection of sensors are evaluated and presented in this study. Similarly, the SnO_2:Agn films are characterized in their structural properties by XRD, the morphology by SEM, chemical analysis by EDS, the topographic and roughness with AFM, the electrical properties by both the two and four probe techniques, and the optical properties by UV-Vis.

2 Experimental methodology

2.1 Thin films synthesis

SnO_2 thin films have been prepared by the sol-gel method and by repeated dip-coating procedure. Also, SnO_2 thin films surface modified with Ag, SnO_2:Agn, were obtained. From tin chloride $SnCl_4{\cdot}5H_2O$ (Merck), a 0.2 M solution was prepared in 2-methoxyethanol, $CH_3OCH_2CH_2OH$ (Merck) and monoethanolamine, $(CH_2CH_2OH)NH_2$ (Merck) (MEA) (Ilican, *et al*., 2008; Thongsuriwong, *et al*., 2013; Jie, *et al*., 2006) and stirred at room temperature around 1 h until a homogeneous and transparent solution was observed. A ratio MEA:Sn fixed of 1.0 was taken. The starting solution in the dark, and at room temperature was aged for seven days before of depositions. Dissolving silver nitrate, $AgNO_3$, in ethanol, CH_3CH_2OH, was prepared a 0.012 M solution, by stirring for 1 h at room temperature, and so the SnO_2 samples were superficially modified. The SnO_2 thin films were grown on of glass substrates soda-lime with a surface section (76 x 26 mm^2) and 1 mm in thickness, previously cleaned and prepared thoroughly.

2.2 Deposition procedure

The coating process by dip-coating method, consisted in dipping and removing the substrate into and from the solution prepared by sol-gel at a speed of 3.3 cm min^{-1}. After each immersion, a drying process at 250 °C in air for 10 min was practiced to the films with the purpose to remove solvents and other organic compounds. This process was repeated until the desired thickness of the sample was reached. A final annealing treatment in air at 250 °C for 1 h was practiced for the samples. Commonly it is reported a heat-treatment at 400 ºC for 1 h or an equivalent (Jie, *et al*., 2006 ; Matshushima, *et al*., 2003; Li, *et al*., 1999). Pure SnO_2 samples and those with surface modified with 1, 3, 5 and 10 Ag layers, films 150 nm order in thickness, were deposited and prepared following the dip-coating procedure.

2.3 Thin films characterization

X-ray diffraction (XRD) patterns of the SnO_2 films, were registered in a MMA model GBC diffractometer using CuK_α (λ = 0.15406 nm) as source of radiation to study the microstructure of the samples, using the $\theta - 2\theta$ technique nearly from 8 to 70º scanning interval

with a 0.02º step; the well-known Scherrer's formula, $D = 0.9\lambda/\beta\cos\theta$, was used in the crystallite size determination. The surface morphology of the films was analyzed in a XL FEG/SFEG/SIRION scanning electron microscope (FEI) and chemical analysis of the films, by electron dispersion energy (EDX) was used, and also the topography of the samples was analyzed by atomic force microscopy (AFM) in a Park AutoProbe CP Equipment (Veeco), the films were analyzed in the contact mode with a Si tip with a constant force k = 0.26 Nm^{-1} and resonant frequency of 40 kHz. The micrographs of cross-section of the films also were registered to obtain the film thickness. The resistance of the samples was obtained using both methods, of two and four point-probe, used for evaluate the sensor responses. The transmittance measurements for the thin films in the visible range, and refractive indices, UV-Vis, were registered with a double beam Perkin Lambda 25 Spectrophotometer, with the substrate as a reference.

3 Results

3.1 X-rays diffraction

For the SnO_2:Agn films with thickness of 150 nm approximately, the X-ray patterns in Fig. 1 correspond to either pure (SnO_2:Ag0) and with 1, 3, 5 and 10 layers of Ag (SnO_2:Ag1, Ag3, Ag5, Ag10) nearly amorphous films. The Bragg peaks at 29.5º and 32.06° are associated to the (111) and (011) planes in the orthorhombic phase of tin oxide (JCPDS No. 24-1342), while the Bragg peaks at 31.83º and 34.3º of the (110) and (101) planes, respectively, to the tetragonal phase of SnO_2 (JCPDS No. 21-1250); the peak position at 2θ = 32.791º (see spectrum of SnO_2:Ag10) corresponds to the plane (111)p of silver oxide (Ag_2O) in accord to the card Code 00-041-1104 (cubic phase). The low crystalline structure of the films is deteriorated as increasing the Ag layers. From the Scherrer's formula, D = $0.9\lambda/\beta\cos\theta$, with λ (0.15406 nm) the wavelength of CuK_α radiation and β is the average width measured at half maximum intensity (FWHM) in radians; the D crystallite sizes resulted approximately in the range 47-69.6 nm for the samples.

3.2 Morphology study

SEM micrographs of SnO_2:Agn representative thin films, are shown in Fig. 2.

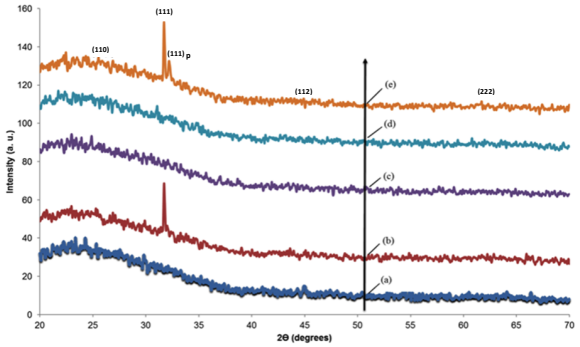

Fig. 1. XRD patterns for (a) SnO_2:Ag0, (b) SnO_2:Ag1, (c) SnO_2:Ag3, (d) SnO_2:Ag5 and (e) SnO_2:Ag10 samples.

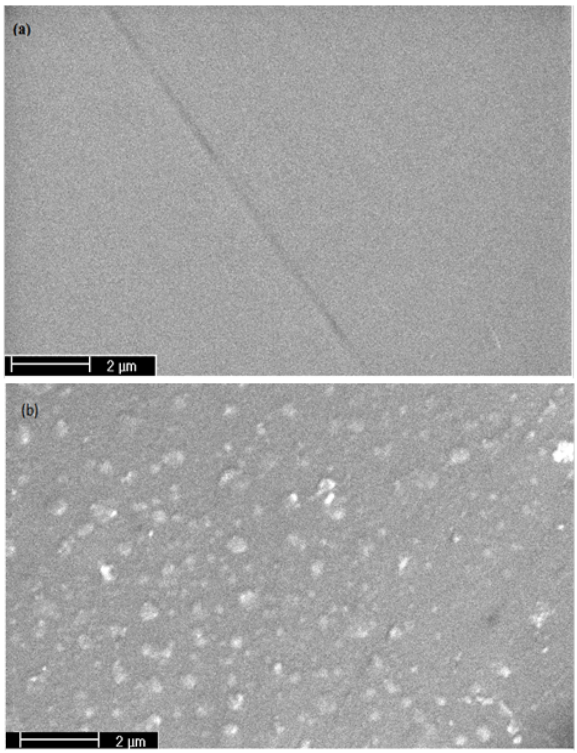

Fig. 2. SEM micrographs of (a) SnO_2:Ag0 and that in (b) SnO_2:Ag5 samples.

The micrograph of SnO_2:Ag0 has a uniform morphology, smooth and without pores apparent as shown (Fig. 2a). On the Fig. 2b for the SnO_2:Ag5 sample, formations of Ag particles or islands can be observed (identified by EDS) with sizes between 20-200 nm; similar formations occur in micrographs of films with several layers of silver (not shown). From the cross section micrographs of SnO_2:Ag0 sample, ~ 150 nm in thickness films, was obtained.

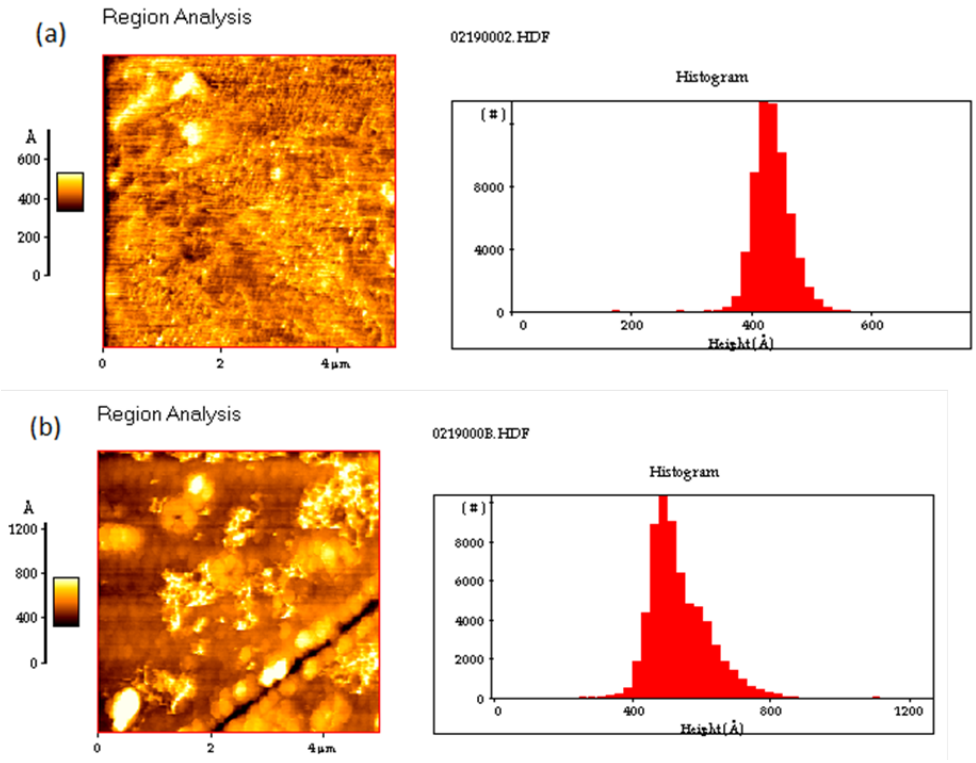

Fig. 3. AFM images and histograms of samples (a) SnO_2:Ag0 and for (b) SnO_2:Ag5.

Table 1. AFM parameters measured for the series of SnO_2:Agn samples.

Samples	Rq (nm)	Ra (nm)	Rm (nm)
SnO_2:Ag0	4.19	2.66	49.4
SnO_2:Ag3	5.4	3.9	45.9
SnO_2:Ag5	9.44	7.11	54.6
SnO_2:Ag10	13.9	10.7	76.7

3.3 Topography study

From a scanned area of (5x5) μm^2 typical AFM images are shown in Fig. 3 ((a) SnO_2:Ag0, and (b) SnO_2:Ag5, samples) with their respective histograms. The roughness parameters of the films, as the root mean square (Rq), the average roughness (Ra), and the maximum height (Rm), were evaluated (Table I). The micrograph of SnO_2:Ag0 has a uniform surface morphology, rough and porous, while the micrograph of SnO_2:Ag5 shows clusters (also shown in SEM), leaving enough surface area exposed; in the SnO_2:Ag10 micrograph (not shown), particles or clusters are present, and a high-surface density of clusters that covers most of the surface area of the film, was observed. From the histograms, the distributions of the grains sizes give, 47.9 and 49.5 nm for SnO_2:Ag0 and that from SnO_2:Ag5 samples, respectively. The grains sizes are in the order like those evaluated from the SEM study.

3.4 Electrical properties

Once the SnO_2 samples were annealed at 250 °C for 1 h, they were stopped and held at room temperature (23 °C) and then the surface resistance was measured by four-probe method, resulting in highly resistive samples (~ GΩ). Subsequently, the tests of gas sensing conducted on each sample, at a given gas concentration and also for a temperature, were measured both the surface resistance and its change by varying the conditions mentioned, by the two-probe method. In general, resistance values of 560 MΩ and their changes were found, and the lowest resistance values resulted in the order of some kΩ. The initial resistance value of 560 MΩ in SnO_2:Agn thin films, remains nearly constant at ambient temperature.

3.5 Optical properties

UV-Vis spectra in the range of 300-1100 nm wavelength were recorded for the SnO_2:Agn (n = 0, 1, 3, 5, 10) samples. The transmittance ($T_{\%}$) between 74 and 80% in the visible window from 450 to 1100 nm for the SnO_2:Agn thin films, resulted as shown (Fig. 4). A sharp absorption edge around 330 nm was found for the SnO_2:Agn thin films. It could say that the number of layers of Ag is reflected in a relative way in the transmittance of the films. A range value of 3.92-4.11 eV for the band width E_g was estimated for the samples; the band width E_g for a direct band semiconductor, is obtained by plotting $(\alpha hv)^2$ vs (hv), with α the absorption coefficient, and extrapolation to the photon energy axis (Ilican, *et al*., 2008; Suchea, *et al*., 2006; Suleimanpour, *et al*., 2011) (Fig. 5), the range of the E_g values estimated for the thin films may reflect uniformity in the process of growth of SnO_2 films and thus a defect density almost unchanged (the XRD peaks positions are not shifted). In SnO_2 films doped with fluorine a value of 4.4 eV around for E_g was reported, slightly higher than that obtained by CVD (Suh, *et al*., 1999). The bandwidth value of E_g obtained in the SnO_2:Agn thin films, presented a shift to the UV side when the surface was modified with various Ag catalyst layers; the opposite occurs when Fe^{3+}, Cu^{2+} ions are incorporated in the matrix of semiconductor TiO_2 on alumina substrates, shifts are obtained in the value of E_g (3.2 eV) to the visible, improving performance of TiO_2 as photo-catalyst in the degradation of pollutants wastewater (Carriazo *et al*., 2014; Luna-Sánchez *et al*., 2013).

From the relationship between the transmittance $T_{\%}$ and the reflectance $R_{\%}$, and the relations of the latter with the refractive index n of the films, themselves given by, $R = (1-T_{\%})/(1+T_{\%})$ and $n = (1+R^{1/2})/(1-R^{1/2})$, one can evaluate the refractive index in the wavelength range recorded in the spectra UV-Vis. The refractive index n as a function of wavelength λ for the films of SnO_2:Agn is plotted in Fig. 6. A significant increase occurs in the refractive indices in the region of short wavelength, and in the range of 400-800 nm the refractive index in the 2.37-2.59 range was registered.

3.6 Sensing properties

The surface resistance in semiconductor thin films is measured using the four-point probe. The two-point probe was used to evaluate the resistance of the films and also its change, when the films are exposed both to the gas pressure and also to the temperature. Semiconductors have different responses to the presence of a gaseous atmosphere, so it is necessary to know the sensitivity available. To know how a sensor device detects a gas, is necessary to evaluate their electrical properties such as resistance R. It is know that the R of a sensor varies with the working temperature T and with the type of gas and its concentration C, and so, to evaluate the sensor response of SnO_2:Agn to the propane gas,

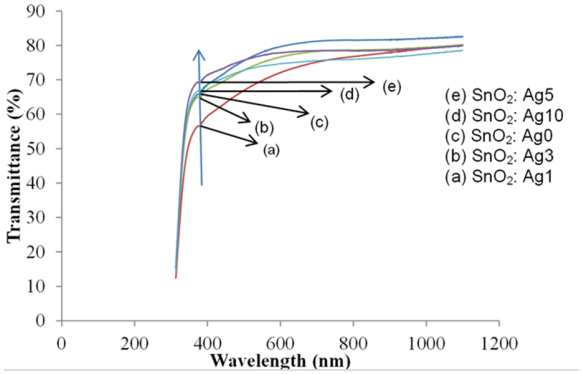

Fig. 4. UV-Vis spectra for the samples of SnO_2:Agn in the 300-1100 nm range.

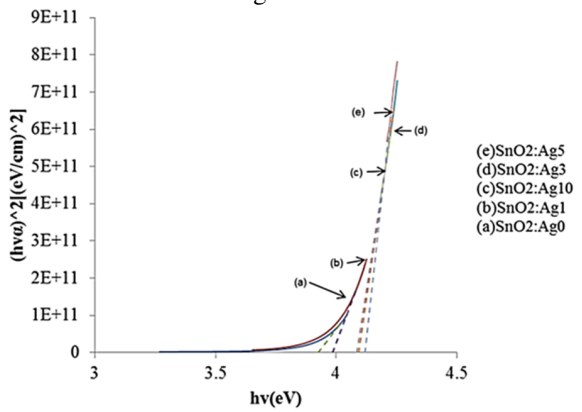

Fig. 5. Method for evaluating the band width *Eg*, for the of SnO_2:Agn samples.

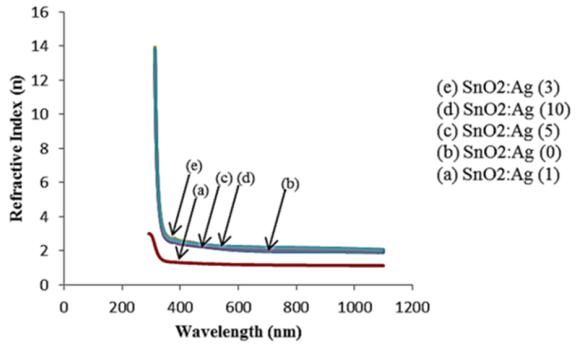

Fig. 6. Graph of the refractive index n against wavelength for the SnO_2:Agn samples.

Table 2. Resistances (MΩ) of the SnO_2:Agn samples.

Samples	SnO_2:Ag:0		SnO_2:Ag:3		SnO_2:Ag:5		SnO_2:Ag:10	
C(ppm)/T(°C)	200	300	200	300	200	300	200	300
0	560	390	550	280	0.55	470	560	360
1	560	370	550	280	0.55	470	560	350
5	560	280	550	250	0.55	420	560	280
50	560	210	540	210	0.54	340	550	200
100	560	133.12	540	189	0.54	220	551	180.53
200	560	112.74	530	180.2	0.53	156.22	480	135.5
300	550	109.61	520	166.24	0.52	107.86	460	113.2
400	550	96.3	520	157.11	0.51	42.34	440	89.19
500	540	74.31	500	136	0.48	0.37	410	50.1

Table 3. Sensitivity matrix at constant concentration, $S(T)_c$.

Samples	SnO_2:Ag0				SnO_2:Ag3				SnO_2:Ag5				SnO_2:Ag10			
C(ppm)/T(°C)	23	100	200	300	23	100	200	300	23	100	200	300	23	100	200	300
0	1	1	1	1.436	1	1	1.018	2.000	1	1.00	1018	1.20	1	1	1.00	1.58
1	1	1	1	1.514	1	1	1.018	2.000	1	1.00	1018	1.20	1	1	1.00	1.04
5	1	1	1	2.000	1	1	1.018	2.240	1	1.00	1018	1.33	1	1	1.00	2.04
50	1	1	1	2.667	1	1	1.037	2.667	1	1.00	1037	1.65	1	1	1.02	2.85
100	1	1	1	4.207	1	1	1.037	2.963	1	1.00	1037	2.55	1	1	1.02	3.16
200	1	1	1	4.967	1	1	1.037	3.108	1	1.02	1056	3.58	1	1	1.17	4.21
300	1	1	1.018	5.109	1	1	1.057	3.369	1	1.02	1077	5.19	1	1	1.22	5.04
400	1	1	1.018	5.815	1	1	1.077	3.564	1	1.04	1098	13.23	1	1.02	1.27	6.39
500	1	1	1.037	7.536	1	1	1.120	4.118	1	1.04	1167	1513	1	1.02	1.37	11.38

the matrices of sensitivity $S(T)_C$, as function of temperature at constant concentration and the sensitivity $S(C)_T$, as function of the concentration and constant temperature, need to be evaluated. If R_C is a reference resistance and that R_i is the resistance of the sensors at a constant concentration of gas, respectively, then the sensitivity in terms of temperature and constant concentration is given by $S(T)_C = R_C/R_i$; similarly, if R_T and R_j are the reference resistance of the sensors and the other for a constant temperature, respectively, the sensitivity as a function of concentration and constant temperature is given by $S(C)_T = R_T/R_j$ (Jie, *et al*., 2006; Li, *et al*., 1999). The resistance values of the sensor SnO_2:Agn for better working conditions, both temperature and to concentration, are presented in Table 2; the elements of the sensitivity matrix $S(T)_C$ are shown in Table 3, while those corresponding to the matrix $S(C)_T$ are not shown.

Fig. 7 graphically shows the sensitivity elements of $S(T)_C$ matrix, of the series of sensors (a) SnO_2:Ag0 and (b) SnO_2:Ag3 depending on operating temperature (23 to 300 °C), for each gas concentration in the range of 0-500 ppm. From 23 to 200 °C the response is low for both series of sensors and are not activated enough in the range of concentrations, but showed the presence of species of oxygen adsorbed on the surface of the sensors, the same reactive with the gas but still has not been promoted sufficient number of charge carriers of the donors to the conduction band of the sensor and/or lack of activation of oxygen vacancies, so that the electrical properties of the sensors would be improved, but as the temperature rises at 300 °C an increasing trend in the responses is shown, there is no saturation of the same. With the increased charge carrier population, the sensitivity of the sensor to the gas is improved. It is also observed that the response of the sensor increases as does the gas concentration; for the activation energy corresponding to the 100 to 300 °C range for the temperatures, when higher the gas concentration so are the reactions that are increased in each case.

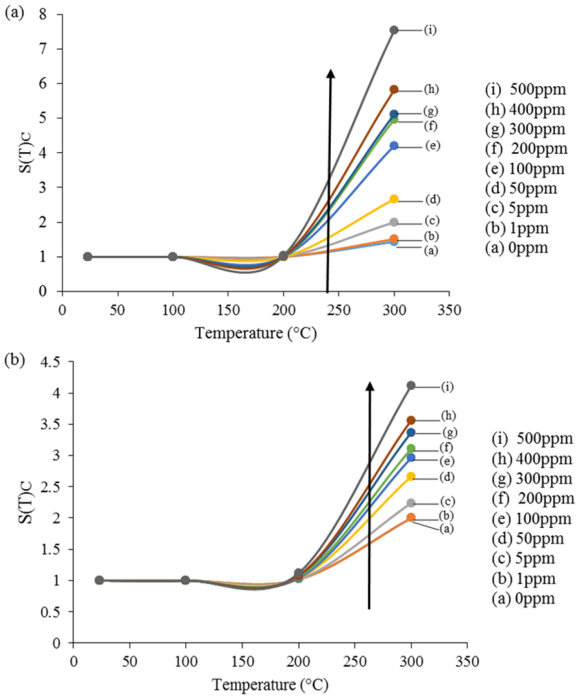

Fig. 7. Sensitivity plots as a function of temperature at constant concentration, $S(T)_C$, of the sensors (a) SnO_2:Ag0 and (b) SnO_2:Ag3 in the range 23-300 °C for operation.

So, 7.5 and 4.12 are the sensitivities at 300 °C for both SnO_2:Ag0 and SnO_2:Ag3 series of sensors, respectively, to 500 ppm. Apparently, the three layers of Ag catalyst play no role in the reactions that take place between oxygen species and the gas, but in the process in which the layers were deposited, the islands of Ag grow and whose distribution and sizes may not be optimal to enforce the role of catalyst in the reactions; on the other hand the pure sensors SnO_2:Ag0, have their surface states, original porosity and roughness with an increased surface area, where the reactions between oxygen species and the gas take place, but with the growth process of Ag islands, the active sites of the pure sensors are diminished and so the response of sensors SnO_2:Ag3 are less than those of the pure ones, the role of the substrate is important.

Graphs Fig. 8(a) and (b), correspond to the series of sensors (a) SnO_2:Ag5 and (b) SnO_2:Ag10 according to the operation temperature and for the gas concentration a constant (0-500 ppm), and where the responses are very different. The response of the series of sensors SnO_2:Ag5, exhibits a maximum around 200 °C for all of them and each of the concentrations, the activation start is at 100 °C, the value of the response remains almost constant (1018-

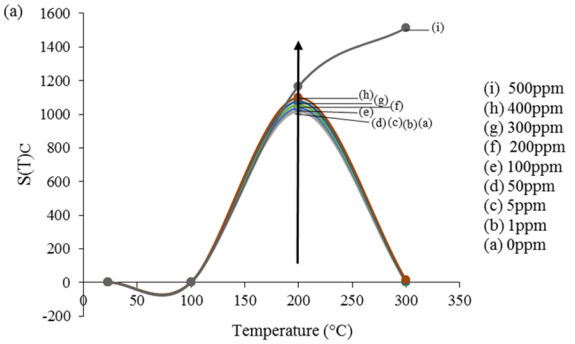

Fig. 8. Sensitivity plots as a function of temperature at constant concentration, $S(T)_C$, of the sensors (a) SnO_2:Ag5 and (b) SnO_2:Ag10 in the range 23-300 °C for operation.

1167) for the range 0-500 ppm and given the difference in response, apparently the gas concentration plays a minor role, as well as that of the islands of the catalyst in the reactions, and with the temperature increase, the response of the series tends to zero at 300 °C; however, the number of sensors SnO_2:Ag5 operating at 300 °C has a slow response at low concentrations, but for 300, 400 and 500 ppm reaches the responses of 5.19, 13.23 and 1513, respectively. The presence of adsorbed oxygen species on active sites of the surface of the semiconductors SnO_2:Ag5 and the same, are activated as the temperature increases from 100 to 200 °C, at the same time the C_3H_8 gas is consumed or is degraded; passing the 200 °C, may be taking off the oxygen species from the surface of the sensor, which participate in the reactions with the gas, or desorption from the surface when increasing temperature, so that one can think that at 200 °C, an equilibrium between both mechanisms are reached and there are no net more charge carriers. However, the responses for the series of sensors SnO_2:Ag10 are different and the elements of sensitivity matrix, $S(T)_C$, in function of temperature and to a constant concentration in the range 0-500 ppm are given in Fig. 8(b). The activation is at 200 °C and is shown where the response increases as increasing both temperature and concentration, so does the response, in fact, 11.4 is the best response at 300 °C and 500 ppm. The behavior is similar to that of the series of sensors of SnO_2:Ag0 and SnO_2:Ag3 in response, as given in Fig. 7. The sensors of SnO_2:Ag10 with ten Ag layers, and where aggregates are formed from grains or islands of the catalyst Ag of different sizes and their own distribution over the surface, decreasing their specific area, both factors may influence the low efficiency of the catalysts, and where catalyst layers cover much of the surface area of

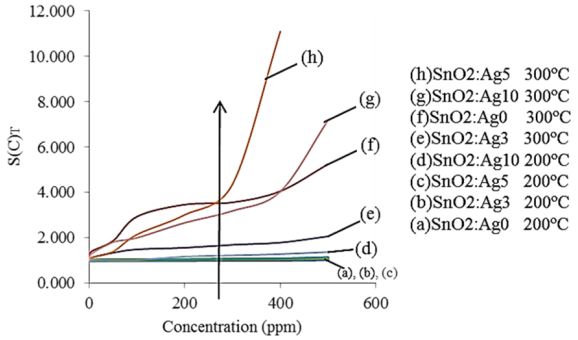

Fig. 9. Plots of the response of some sensors SnO_2:Agn operating at 200 and 300 °C, and the same correspond to the respective elements in the matrix $S(C)_T$.

the pure SnO_2 and blocks the active sites that anchor the species of oxygen that react with the gas. One would expect from the series of SnO_2:Ag10, with its ten surface layers of catalyst and longer exposure time at 250 °C with the final treatment, a better efficiency.

To display the response presented by the sensors operating at constant temperature and varying the concentration 0-500 ppm, the elements of the sensitivity matrix, $S(C)_T$, are presented in graphical form for sensors SnO_2:Agn, see the Fig. 9. Some sensors operating at 200 and 300 °C and varying the concentration over the range of 0-500 ppm were selected. In the chart, two groups of sensors are identified, those operating at 200 °C which have a decreased response when increasing the gas concentration in the 0-500 ppm range, and the second group operating at 300 °C with best responses with increasing concentration; it is shown that the sensors respond to 0-500 ppm in gas concentration, and it generally increases as the gas concentration does, so the signal increases. The responses of SnO_2:Ag0, were 1.02 and 4.05 to 400 ppm and only 1.04 and 5.25 to 500 ppm, operating at 200 and 300 °C, respectively. The values of 4.04 and 7.2 to 400 and 500 ppm, respectively, correspond to the SnO_2:Ag10 sensors operating at 300 °C and the response increases with concentration. Operating at 300 °C the series of SnO_2:Ag5 have the best values for the sensitivity matrix elements, $S(C)_T$, that is, 4.36, 11.10 and 1270 for 300, 400 and 500 ppm in gas concentration, respectively, the signal generally increases as the concentration increases; to an activation energy of 300 °C the sensitivity of the SnO_2:Ag5 increases with the C_3H_8 gas concentration, but not proportional to the number of the Ag layers.

4 Discussion

On the interface of the semiconductor SnO_2:Agn, oxygen species are adsorbed (O_2, O_2^-, O^-) (Kiss, *et al*., 2001; Haridas, *et al*., 2008; Jie, *et al*., 2006; Gong, *et al*., 1999; Kanamori, *et al*., 1999) and once decoupled, they are dispersed over the entire surface of the semiconductor, finding attachment sites and drawing electrons from the semiconductor SnO_2:Agn and hence charge carriers thinning regions near the surface. However, by exposing the semiconductor interface SnO_2:Agn to the reducing gas, C_3H_8, and where their molecules are dissociated and dispersed on the surface of metal oxide and also over the islands of the catalyst Ag formed on the metal oxide, and of the charges coming from the different donors and from oxygen vacancies (v^{--}), that are activated because the temperature and so enabling the reaction of propane gas with oxygen species (Haridas, *et al*., 2008; Kanamori, *et al*., 1999). Catalyst islands can dissociate gas molecules, which are dispersed over the entire surface of the interface of the devices, SnO_2:Agn, facilitating reactions such as: $C_3H_8 + 2O^- \rightarrow H_2O + C_3H_6\text{-}O + e^-$(Haridas, *et al*., 2008), until the mineralization is reached or the gas degraded, increasing the charge carriers density and due to the reaction between the oxygen species and the gas, reducing the sensors resistance of the SnO_2:Agn and thus its sensitivity to the test gas, increases. Of course, the activation energy for such reactions carried out, come from the operating temperature of the sensors and the gas concentration, and type of the gas exposed to the sensors interface of SnO_2:Agn. By the method of growth of the films, they resulted to be non-stoichiometric, also amorphous, sizes of different grains, different stress states and defects due to the different times of exposure to the temperature of 250 °C and the final heat treatment, the low temperature in the synthesis of the films was a starting experimental condition. Then, they have different sizes and grain boundaries (potential barriers), oxygen vacancy concentration (v^{--}) and surface states; when the density of the charge carriers in between two grains is high, the inter-grain barrier height is decreased and as a consequence the tunneling is possible and so the sensors resistance of the SnO_2:Agn can be low and thus a high sensitivity to the gas (Chizhov *et al*., 2014). When the sensor tests are carried out upon exposure to different temperatures, in addition to activated oxygen species such as O_2^-, O^-, which are the most common (Kiss, *et al*., 2001; Haridas, *et al*., 2008; Jie, *et al*., 2006; Gong, *et al*., 1999;

Kanamori, *et al*., 1999), and wherein the amount of each of the species depends on the temperature, being the most favored for high temperature the O^- species (Koziej, *et al*., 2007), so from the O_2^- oxygen species on the SnO_2:Agn surface and an electron e^- promoted by the temperature in the 100-300 °C range, is possible the reaction: $O_2^- + e^- \rightarrow 2O^-$, so the electron trapped by the oxygen ion, O_2^-, can return to the surface of SnO_2:Agn, and so decreasing the resistance as happen to TiO_2 nanorods sensors (Yang *et al*., 2014), and therefore explanation will be possible especially for each series of sensors prepared and studied in this work. Thus, when the operating temperature of a sensor is increased, the charge carrier concentration of the semiconductor increases, but also the oxygen vacancies near the surface of the sensors, SnO_2:Agn (Kanamori, *et al*., 1999). With such increase in temperature, charge carrier concentration, increases, and hence the resistance of the sensor in the presence of the gas, decreases, and so does the sensitivity of the sensor (Koziej, *et al*., 2007; Kiss, *et al*., 2001; Li, *et al*., 1999). Thus, the increase in carrier electron concentration of the sensor SnO_2:Agn and depending on that increase, and so will be the mechanisms involved in the reactions; also it is necessary to know the preparation methods and synthesis of the thin films, the precursors used, of the interface characteristics, the electrical properties, the type and the gas concentration, the operating temperature, and many others. From the study carry out of the thin films SnO_2:Agn it has given a plausible explanation of the response for the sensors and their sensitivity to propane gas. Many factors are involved in the possible mechanisms of interaction between oxygen species and the type of gas, but it requires special study skills (Schmid, *et al*., 2003; Schmid, *et al*., 2004).

Conclusions

The series of SnO_2:Agn in thin film have been successfully prepared by the sol-gel technique and dip-coating procedure, and were studied. A series of samples of approximately 150 nm thickness resulted. The samples SnO_2:Agn were characterized. The structure was amorphous although achieved define diffraction planes associated with orthorhombic and tetragonal phases of SnO_2, from which a crystal size in the 47-69.6 nm range, and also the Ag_2O phase, were registered. The morphology of the films was recorded without cracks and uniform and also over the modified films the nanoparticles or islands of Ag (EDS study) distributed on film surface (SEM) were recorded, and topography showed grain sizes in the range 47.9-49.5 nm, consistent with the results of X ray. The resistive semiconductor films were relatively transparent and with a bandwidth in the range 3.92-4.11 eV. Its properties as propane gas sensors were studied and possible mechanisms of reaction between the sensor and gas were proposed.

The characterization of the samples carry out, shown to be excellent for detecting C_3H_8 gas. The best responses of the sensors resulted at high operating temperatures and higher concentrations of the gas. Also, the responses of the sensors when is varying the concentration of gas, and the operating temperature but constant, increase with increasing the gas concentration. The sensor arrays with five layers of catalyst Ag, increased their response until three orders of magnitude respect to the response of pure sensors, and the overall results, are above what is reported in literature even when compared to studies conducted in Pt, Ag and others, deposited on SnO_2 films. However, more study is required to optimize several experimental parameters.

Acknowledgement

Author thanks to the SIP-IPN: 20141245 Proyect, to F.J. Camacho and N. Tirado for technical assistance.

References

Álvarez-Amparán M. A. and Cedeño Caero L. (2014). Efecto del hidroperóxido de cumeno sobre la desulfuración oxidativa. *Revista Mexicana de Ingeniería Química 13*, 787-797.

Carriazo J. G., Ensuncho-Muñoz A. and Almanza O. (2014). Electron paramagnetic resonance (EPR) investigation of TiO_2-delaminated clays. *Revista Mexicana de Ingeniería Química 13*, 473-481.

Chizhov A. S., Rumyantseva M. N., Filatova D. G., Drozdov K. A., Krylov I. V., Abakumov A. M. and Gaskov A. M. (2014). Visible light activated room temperature gas sensors based on nanocrystalline ZnO sensitized with CdSe quantum dots. *Sensors and Actuators B 205*, 305-312.

Colín-Luna J. A., Medina-Mendoza A. K., De los Reyes J. A., Escobar J., Montoya de la Fuente J.

A. and Suárez P. R. (2013). Efecto de la relación Si/Al en la hidrodesulfuración profunda de catalizadores Pt/Al-MCM41. *Revista Mexicana de Ingeniería Química 12*, 271-282.

Fort A., Mugnaini M., Rocchi S., Serrano-Santos M. B., Vignoli V. and Spinicci R. (2007). Simplified models for SnO_2 sensors during chemical and thermal transients in mixtures of inert, oxidizing and reducing gases. *Sensors and Actuators B 124*, 245-259.

Gong H., Wang Y. J., Teo S. C. and Huang L. (1999). Interaction between thin-film tin oxide gas sensor and five organic vapors. *Sensors and Actuators B 54*, 232-235.

Haridas D., Sreenivas K. and Gupta V. (2008). Improved response characteristics of SnO_2 thin film loaded with nanoscale catalysts for LPG detection. *Sensors and Actuators B 133*, 270-275.

Ilican S., Caglar Y. and Caglar M. (2008). Preparation and characterization of ZnO thin films deposited by sol-gel spin coating method. *Journal of Optoelectronics and Advanced Materials 10*, 2578-2583.

Jie Z., Li-Hua H., Shan G., Hui Z. and Jing-Gui Z. (2006). Alcohols and acetone sensing properties of SnO_2 thin films deposited by dip-coating. *Sensors and Actuators B 115*, 460-464.

Kanamori M., Susuki K., Ohya Y. and Takahashi Y. (1994). Analysis of Change in the Carrier Concentration of SnO_2 Thin Film Gas Sensor. *Japan Journal Applied Physics 33*, 6680-6683.

Kappler J., Tomescu A., Barsan N. and Weimar U. (2001). CO consumption of Pd doped SnO_2 based sensors. *Thin Solid Films 391*, 186-191.

Kennedy M. K., Kruis F. E., Fissan H., Nienhaus H., Lorke A. and Metzger T. H. (2005). Effect of in-flight annealing and deposition method on gas-sensitive SNO_x films made from size-selected nanoparticles. *Sensors and Actuators B 108*, 62-69.

Kiss G., Pintér Z., Perczel I. V., Sassi Z. and Réti F. (2001). Study of oxide semiconductor sensor materials by selected methods. *Thin Solid Films 391*, 216-223.

Koziej D., Thomas K., Barsan N., Thibault-Starzyk F. and Weimar U. (2007). Influence of annealing temperature on the CO sensing mechanism for tin dioxide based sensors-Operando studies. *Catalysis Today 126*, 211-218.

Li, G.-J., Zhang X.-H. and Kawi S. (1999). Relationships between sensitivity, catalytic activity, and surface areas of SnO_2 gas sesnors. *Sensors and Actuators B 60*, 64-70.

Luna-Sánchez R. A., Zermeño-Reséndiz B. B., Moctezuma E., Contreras-Bermúdez R. E., Leyva E. and López-Barragán M. A. (2013). Fotodegradación de omeprazol en solución acuosa utilizando TiO_2 como catalizador. *Revista Mexicana de Ingeniería Química 12*, 85-95.

Maldonado A., Mallén-Hernández S. A., Vega-Pérez J., Olvera M. de la L. and Tirado-Guerra S. (2009). Chromium doped zinc oxide thin films deposited by chemical spray used in photo-catalysis and gas sensing. *Revista Mexicana de Física S 55*, 90-94.

Maldonado A., Mallén-Hernández S. A., Tirado-Guerra S. and Olvera M. de la L. (2010). Titanium dioxide thin films deposited by the sol-gel technique starting from titanium oxy-acetyl acetonate: gas sensing and photocatalyst applications. *Phys. Status Solidi C 7*, No. 9, 2316-2320.

Matsushima Y., Nemoto Y., Yamazaki T., Maeda K. and Suzuki T. (2003). Fabrication of SnO_2 particle-layer on the glass substrate using electrospray pyrolysis method and the gas sensitivity for H_2. *Sensors and Actuators B 96*, 133-138.

Padilla J. M., del Ángel G., Bertin V., Cortés-López A. J., Fierro J. L. G. and Poisot M. (2013). Combustión de tolueno en catalizadores de Pd y Pt soportados en γ-Al_2O_3 y γ-Al_2O_3-Ce. *Revista Mexicana de Ingeniería Química 12*, 73-83.

Safanova O. V., Rumyantseva M. N., Ryabova L. I., Labeau M., Delabouglise G. and Gaskov A. M. (2001). Effect of combined Pd and Cu doping on microstructure, electrical and gas sensor properties of nanocrystalline tin dioxide. *Materials Science and Engineering B 85*, 43-49.

Sahner K., Schonauer D., Matam M., Post M., and Moos R. (2008). Selectivity enhancement of p-type semiconducting hydrocarbon sensors-The use of sol-precipitated nano-powders. *Sensors and Actuators B 130*, 470-476.

Schmid W., Bârsan N. and Weimar U. (2003). Sensing of hydrocarbons with tin oxide sensors: possible reaction path as revealed by consumption measurement. *Sensors and Actuators B 103*, 232-236.

Schmid W., Bârsan N. and Weimar U. (2004). Sensing of hydrocarbons and CO in low oxygen conditions with tin dioxide sensors: possible conversion path. *Sensors and Actuators B 103*, 362-368.

Shinde V. R., Gujar T. P. and Lokhande C. D. (2007). LPG sensing properties of ZnO films prepared by spray pyrolysis method: Effect of molarity of precursor. *Sensors and Actuators B 120*, 551-559.

Amornpitoksuk P. and Suwanboon S. (2013). Structure, morphology, photocatalytic and antibacterial activities of ZnO thin films prepared by dip-coating method. *Advanced Powder Technology 24*, 275-280.

Soleimanpour A. M., Hou Y. and Jayatissa A. H. (2011). The effect of UV irradiation on nanocrystalline zinc oxide thin films related to gas sensing characteristics. *Applied Surface Science 257*, 5398-5402.

Suchea M., Christoulakis S., Moschovis K., Katsarakis N. and Kiriakidis G. (2006). ZnO transparent thin films for gas sensor applications. *Thin Solid Films 515*, 551-554.

Suh S., Zhang Z., Chu W. K. and Hoffman D. M. (1999). Atmospheric-pressure chemical vapor deposition of fluorine-doped tin oxide thin films. *Thin Solid Films 345*, 240-243.

Yang H-Y., Cheng X-L., Zhang X-F., Zheng Z-K., Tang X-F., Xu Y-M., Gao S., Zhao H. and Huo L-H. (2014). A novel sensor for fast detection of triethylamine based on rutile TiO_2 nanorods arrays. *Sensors and Actuators B 205*, 322-328.